MIT Open Access Articles

Near infrared spectroscopic assessment of developing engineered tissues: correlations with compositional and mechanical properties

Massachusetts Institute of Technology

Near Infrared Spectroscopic Assessment of Developing Engineered Tissues: Correlations with Compositional and Mechanical Properties

Arash Hanifi[*,1], **Uday Palukuru**[*,1], **Cushla McGoverin**[1], **Michael Shockley**[1], **Eliot Frank**[2], **Alan Grodzinsky**[2], **Richard Spencer**[3], and **Nancy Pleshko**[1,‡]

[1]Department of Bioengineering, Temple University, Philadelphia, PA

[2]Department of Biological Engineering, Massachusetts Institute of Technology, Cambridge, MA

[3]National Institute on Aging, National Institutes of Health, Baltimore, MD

Abstract

Articular cartilage degeneration causes pain and reduces the mobility of millions of people annually. Regeneration of cartilage is challenging, due in part to its avascular nature, and thus tissue engineering approaches for cartilage repair have been studied extensively. Current techniques to assess the composition and integrity of engineered tissues, including histology, biochemical evaluation, and mechanical testing, are destructive, which limits real-time monitoring of engineered cartilage tissue development in vitro and in vivo. Near infrared spectroscopy (NIRS) has been proposed as a non-destructive technique to characterize cartilage. In the current study, we describe a non-destructive NIRS approach for assessment of engineered cartilage during development, and demonstrate correlation of these data to gold standard mid infrared spectroscopic measurements, and to mechanical properties of constructs. Cartilage constructs were generated using bovine chondrocyte culture on polyglycolic acid (PGA) scaffolds for six weeks. BMP-4 growth factor and ultrasound mechanical stimulation were used to provide a greater dynamic range of tissue properties and outcome variables. NIR spectra were collected daily using an infrared fiber optic probe in diffuse reflectance mode. Constructs were harvested after three and six weeks of culture and evaluated by the correlative modalities of mid infrared (MIR) spectroscopy, histology, and mechanical testing (equilibrium and dynamic stiffness). We found that specific NIR spectral absorbances correlated with MIR measurements of chemical composition, including relative amount of PGA (R = 0.86, p = 0.02), collagen (R = 0.88, p = 0.03), and proteoglycan (R = 0.83, p = 0.01). In addition, NIR-derived water content correlated with MIR-derived proteoglycan content (R = 0.76, p = 0.04). Both equilibrium and dynamic mechanical properties generally improved with cartilage growth from three to six weeks. In addition, significant correlations between NIRS-derived parameters and mechanical properties were found for constructs that were not treated with ultrasound (PGA (R = 0.71, p = 0.01), water (R = 0.74, p = 0.02), collagen (R = 0.69, p = 0.04), and proteoglycan (R = 0.62, p = 0.05)). These results lay the groundwork for extension to arthroscopic engineered cartilage assessment in clinical studies.

[‡]Corresponding author: Nancy Pleshko, PhD, 1947 N. 12th Street, Philadelphia, PA 19122, npleshko@temple.edu; 215-204-4280.
[*]These authors contributed equally to the manuscript

Graphical Abstract

Non-destructive near infrared spectroscopic data can be utilized for assessment of compositional and mechanical properties of engineered cartilage.
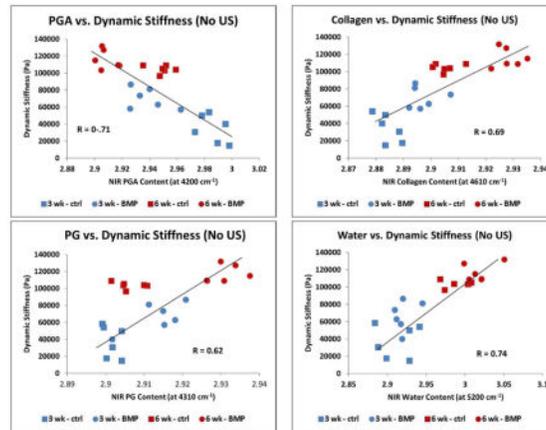
Introduction

Articular cartilage degeneration is characterized in part by alterations in cartilage matrix macromolecular composition and structure, including loss of proteoglycans and changes in tissue water content.[1, 2] These processes may progress to outright disease accompanied by pain and functional limitations.[3, 4] Cartilage lacks a significant degree of self-repair, due to its limited blood supply, relatively low cellularity, and the relatively modest synthetic capacity of chondrocytes, the sole cell type within cartilage.[5–7] Partly for these reasons, current interventions for cartilage repair display limited long-term success[89] and often result in the production of fibrocartilage rather than the more functional hyaline cartilage phenotype. In addition, these techniques may require tissue harvesting followed by ex vivo tissue development and reimplantation, resulting in the need for two surgical procedures.[9–13] Therefore, there continues to be a pressing need for development of further therapeutic modalities for degenerative cartilage disease.

Interventions based on engineered cartilage tissue remain the focus of a great deal of research.[10, 14–17] The quality of engineered cartilage can be affected by a wide variety of factors such as source of cells and scaffolds characteristics[18], the effects of which have been explored using biodegradable polymeric scaffolds such as polyglycolic acid (PGA).[19–22] Addition of growth factors has been shown to enhance cartilage regeneration by promoting chondrogenesis,[23–26] increasing chondrogenic differentiation of mesenchymal stem cells, and increasing the expression of cartilage matrix components including type II collagen and aggrecans.[27] Mechanical stimulation via hydrostatic pressure [17] or ultrasound [28–30] has also been shown to augment matrix production from chondrocytes, with these effects having been shown to be further augmented in certain circumstances by the addition of BMP-2 and BMP-4.

However, while there are multiple potential interventions to modulate growth, the options for molecular-level assessment of engineered cartilage during development are highly limited, so that it remains difficult to implement appropriate growth condition changes during construct development. Histology and immunohistochemistry, [31, 32] biochemical assays,[33, 34] X-ray and computed tomography (CT),[35, 36] magnetic resonance imaging (MRI),[37, 38] and mechanical testing [39, 40] have all been used, but these techniques are either destructive[41–46] or lack adequate molecular specificity.[47–50]

Infrared spectroscopic techniques for evaluation of engineered cartilage have been developed in part to address this need. Mid infrared (MIR) spectroscopic methods provide compositional information,[51–53] but are restricted to near-surface evaluation due to the limited penetration depth, ~5–10 μm, of the MIR radiation. To address this limitation, an emerging alternative is the application of near infrared spectroscopy (NIRS), generally applied to tissue via a fiber optic probe, which makes use of shorter-wavelength radiation than does MIR. This results in a substantial increase in penetration depth to centimeters, permitting full-thickness analysis of engineered cartilage.[54, 55] Recent NIR studies of cartilage composition have successfully evaluated water content [56] and cartilage matrix molecular components such as proteins and sugars.[54, 57–60] Baykal et al. assessed molecular composition of harvested engineered cartilage using NIRS,[59] and Palukuru et al. developed a model based on NIRS to predict cartilage tissue composition.[60] Most recently, we described a nondestructive NIRS fiber optic technique for evaluation of engineered cartilage, and demonstrated correlations of NIRS data to destructive biochemical measurements [61]. In that earlier study, chondrocytes were seeded onto polyglycolic acid (PGA) scaffolds, with no growth factors or mechanical stimulation applied, and monitored spectroscopically for 6 weeks. In the current study, we applied non-destructive NIR fiber optic assessment to development of engineered cartilage in the presence of growth factors and mechanical stimulation, and investigated correlations of NIR spectral data to gold standard MIR chemical data and mechanical properties.

Materials and Methods

Chondrocyte Isolation

Articular cartilage samples (~2 mm^3) were harvested from the femoropatellar groove and femoral condyles of 1–3 week old bovine stifle joints within 24 hours of slaughter (Research 87, Boylston, MA). Tissue was digested in a spinner flask containing 200 ml Dulbecco's modified eagle medium (DMEM), 250 units/ml of collagenase type II, 100 units/ml of penicillin, 100 μg/ml of streptomycin and 100 μg/ml of fungizone (Invitrogen Life Technologies, Gaithersburg, MD). Primary chondrocytes were isolated after 14 hours of digestion. The cell suspension was filtered through 70 μm sterile nylon filters to separate debris, pelleted at 1000g and reconstituted with 1X phosphate buffered saline (PBS) (Invitrogen Life Technologies, Gaithersburg, MD). Cell number was assessed using a hemocytometer.

Tissue Culture

Scaffolds of 2-mm thickness and 5 mm diameter (Modified Polymer Components, Sunnyvale, CA) were cut from non-woven PGA felt using a biopsy punch (n=48). The PGA disks were sterilized using 100% ethanol, washed in sterile 1X PBS, and allowed to air dry. Chondrocytes were then pre-cultured on PGA scaffolds (20×10^6 cells/scaffold) using a spinner flask for 72 hours in a growth factor-free culture medium [DMEM, 10% Fetal bovine serum, 2 mM L-glutamine, 50 μg/ml of gentamicin, 0.1 mM non-essential amino acids, 0.4 mM L-proline 50 μg/ml of L-ascorbic 2-phosphate (Invitrogen Life Technologies, Gaithersburg, MD), and the same antibiotics as above]. Seeded scaffolds were transferred into 6-well glass-bottom cell culture dishes (In Vitro Scientific, Sunnyvale, CA) with media changes performed three times per week. Glass bottom cell culture dishes were used since they do not exhibit interfering NIR absorbances. Half of the constructs (n=24) received 5ml of culture media per construct supplemented with 50 ng/ml of BMP-4 (BMP-4 group). The remaining constructs received 5ml per construct of regular culture media (Control group). Constructs were cultured in an incubator at 37°C, 100% relative humidity and 5% CO_2.

To provide a potential augmentation of the anabolic effects of BMP-4, mechanical stimulation via pulsed low intensity ultrasound (PLIUS) was applied to six constructs in each of the Control and BMP-4 groups and designated Control/US and BMP-4/US,[50] Briefly, PLIUS was applied thorough the FDA-approved Exogen 4000+ device (Smith & Nephew, Inc.), operating at a carrier frequency of 1.5 MHz, burst frequency of 1 kHz, burst width of 200 ms, and spatial-average temporal-average output intensity of 30 mW/cm^2. The signal was transmitted via coupling gel to the constructs through the bottom of the well plate. Constructs were treated 5 days per week for 20 min for either three or six weeks. BMP-4 and PLIUS stimulation were provided to potentially augment the dynamic range of construct growth and properties, with the combination of these two modalities expected to show the greatest effect. Sample group and number are detailed in Table 1.

NIRS Data Collection

NIR spectral data (8000–4000 cm^{-1}) were collected from the constructs during each media change when they were not submersed in the culture medium (to reduce the amount of water interference). Acquisition was performed using a diffuse reflectance silica glass NIR fiber optic probe (10 mm probe head; inner diameter of transmitting and receiving fiber groups 3.5 mm; Remspec Corp, Charlton, MA) connected to a Bruker (Billerica, MA) Matrix F spectrometer. Three spectra per sample were collected at 16 cm^{-1} spectral resolution with 128 co-added scans. The fiber optic was held 1 mm away from the tissue for all data collection.

Tissue Harvesting

One set of cartilage constructs was harvested after three weeks of incubation, with another set harvested after six weeks. Constructs were washed in PBS, weighed to obtain whole sample wet weight, and bisected. One half was frozen at −20°C in a solution containing 1X PBS and protease inhibitor and retained for mechanical testing. The other half was fixed in 10% formalin (24 hours), washed three times in 1X PBS, and processed for paraffin

embedding. Embedded samples were sectioned and used for mid infrared (MIR) and histology analysis.

MIR and Histology

Paraffin-embedded constructs were sectioned at 6 μm onto low-e slides (Kevley Technologies, Chesterland, OH) for MIR spectral imaging (three sections per construct), and onto plus microscope slides to enhance tissue adhesion for histology. Sections were subsequently deparaffinized and rehydrated using graded xylene and ethanol washes. MIR spectral imaging data were collected using a Spotlight 400 Imaging Spectrometer (Perkin Elmer, Waltham, MA) in the 4000–780 cm^{-1} range with spectral resolution of 8 cm^{-1} and pixel resolution of 25 μm with 2 co-added scans.

Histologic tissue sections were co-stained with Alcian blue to visualize proteoglycans, and haematoxylin and eosin (H&E) to identify cells and ECM. Tissue sections were imaged using an inverted microscope (Nikon Instruments, Melville, NY).

MIR Spectral Data Analysis

MIR spectral imaging data were analyzed using ISys 5.0 software (Malvern Instruments, Columbia, MD). Raw spectra were processed using a multiplicative signal correction (MSC) and converted to second derivative spectra to resolve underlying peaks and correct for baseline offsets. A 13 point Savitzky-Golay smoothing was applied, and spectra inverted by multiplication by −1 to convert to positive peak heights. The 1748 cm^{-1} C=O stretching vibration of PGA was used to map the distribution of PGA throughout the construct.[62] Construct collagen content was evaluated using the 1336 cm^{-1} peak that arises from the CH$_2$ side chain vibration in collagen.[51, 63] The peak at 1152 cm^{-1}, reflecting C-O-C ring vibrations of sugars, corresponds to the concentration of PG in cartilage[64, 65] and was used to map the distribution of PG. The total amount of each component in the tissue was obtained by summing the pixel-wise product of peak amplitudes to obtain the total amount of PGA, collagen or PG for each construct. Spectral data from three tissue sections per construct were averaged for quantification.

NIR Data Analysis

NIR spectra were analyzed using Unscrambler X (CAMO Software, Oslo, Norway). Three spectra per construct were collected and averaged at each timepoint, and then processed with an extended multiplicative scatter correction (EMSC) [66], followed by area normalization. Second derivative processing was performed with a 41 point Savitzky-Golay smoothing window, [67] with shorter windows resulting in inadequate noise filtering (data not shown). Inverted second derivative peak heights at 5200 cm^{-1} were used to define water content,[56] NIR absorbances at 4610 cm^{-1} and 4310 cm^{-1} were used as a measure of collagen and PG content, respectively,[60] while the 4200 cm^{-1} absorbance, unique to PGA,[68] was used to assess PGA degradation.

Mechanical Measurements

Frozen constructs were allowed to thaw at room temperature prior to mechanical testing, which was performed under unconfined compression in PBS containing protease inhibitors.

Construct wet weight and thickness were measured, with effective area computed as wet weight (an approximation of volume) divided by thickness in order to calculate stress and strain from the applied displacement and resultant load. Compressive strain measurements were performed with successive ramped strains of 5%, 10%, 12.5% and 15%, each applied over 60 seconds and maintained for 8–10 min to permit equilibration of stress. A series of 1% peak-to-peak sinusoidal compressive strains was then applied over a range of frequencies from 2 to 0.005 Hz. Equilibrium stiffness was computed as the slope of the equilibrium stress-strain values at 10%, 12.5%, and 15% strain. Dynamic stiffness was computed as the peak-to-peak stress amplitude divided by the peak-to-peak strain amplitude at 0.01 Hz, 0.1 Hz, and 1 Hz frequencies. These parameters have previously been established as appropriate for evaluation of mechanical properties of cartilage in the physiological range.[69–71] Dynamic stiffness measurements were essentially independent of frequency, so that we show results only shown for 0.1 Hz.

Following mechanical testing, the engineered cartilage constructs (half of original construct) were lyophilized for 72 hours to permit measurement of dry weight. Percent water was calculated as:

$$Percent\ Water = (Wet\ Weight - Dry\ Weight)/Wet\ Weight * 100$$

Statistical Analysis

Correlations between NIR-derived matrix components, and molecular and mechanical properties were quantified by the Pearson correlation coefficient. Due to use of different halves of the construct for MIR and dry weight measurements, water content, which depends on dry weight of the entire construct, could not be calculated. Therefore, NIR-derived water content could not be correlated to the water content of the intact constructs. Differences in mean values of NIR, MIR and mechanical data were assessed by two way ANOVA, with treatment category and time as independent variables, followed by Tukey posthoc comparisons with significance defined as p 0.05. Calculations were performed using Sigmaplot 12.0 (Sysstat Software, San Jose, CA).

Results

Tissue Development – Function of Time and Treatment

Engineered cartilage constructs showed a visible color change from red (3 weeks) to light pink (6 weeks), likely due to a decrease in the relative amount of media retained in the construct (Figure 1). Longer culture time significantly increased construct wet weight for BMP-4 and BMP-4/US treated groups (Figure 2A); however, no significant increase was seen in the wet weight of Control or US-treated samples during development. Construct percentage water content was significantly lower at week 6 compared to week 3 for the BMP-4/US group. This is likely due to increasing tissue matrix components (Figure 2B). All sample groups showed a significant increase in volume from week 3 to week 6, while the increase in sample thickness over time was not significant for any group (Figure 2C and 2D).

Histological Evaluation

Alcian blue and H&E co-stained engineered cartilage tissue sections demonstrated a generally widespread distribution of proteoglycan, except for in the interior where residual PGA was observed, particularly at the three week timepoint (Figure 3). The PGA fibers qualitatively diminished from 3 to 6 weeks in Control and Treated groups.

There was an absence of zonal organization in the constructs, which was not surprising, given that constructs were grown under conditions without defined directionality. Large numbers of cells seeded and proliferated inside the engineered constructs in Control and treated groups at both harvest time points. However, the morphology of the cells differed somewhat with respect to position within the scaffold, with cells on the periphery more flattened and elongated compared to interior cells (Figure 3). This may indicate a degree of de-differentiation of the peripheral cells to the fibroblast phenotype, possibly due to a different degree of cellular conditioning between the more inner and more peripheral tissue zones (Figure 3). Consistent with this is the denser H&E staining in the peripheral regions (red purple vs. blue staining), particularly for the 6-week constructs, and a relatively greater amount of fibrous tissue. This may also be indirectly indicated by the less dense peripheral Alcian blue staining.

MIR Compositional Data

MIR spectra from regions of constructs with and without residual PGA are shown in Figure 4. The presence of residual PGA fibers resulted in scattering artifacts just above the 1748 cm^{-1} absorbance, but were limited to that spectral region. Consistent with the PG distribution visualized in the Alcian blue staining, MIR-derived PG is evident throughout the constructs, with the exception of interior regions dominated by residual PGA (Figure 3). This reinforces the notion that the constructs consist primarily of hyaline, as opposed to fibro, cartilage. MIR permits a more quantitative assessment of macromolecular concentration. Spectroscopic analysis indicated that, as suggested by histology staining, collagen content was greater towards the periphery of the constructs, to an extent that increased with time in culture (Figure 3).

MIR data also demonstrated the overall decrease in PGA content from 3 to 6 weeks. In addition, groups treated with BMP-4 showed a reduced amount of PGA content compared to the Control group at three weeks (Figure 3 and Figure 5A). Collagen increased from 3 weeks to 6 weeks (Figure 5B). The highest collagen content was observed for the BMP-4/US treated samples after six weeks of tissue culture. A similar pattern was observed for the PG content of engineered constructs and PG increased from 3 weeks to 6 weeks. Among treated samples, the six week BMP-4 and BMP-4/US treated groups showed a significant increase in PG compared to the three week samples with the same treatment (Figure 5C). Overall, in the BMP-4/US group, all components including PGA, collagen, and PG changed significantly compared to the 3 week Control group.

Non-destructive NIRS Compositional Assessment

Second derivative processing of the NIR spectra revealed enhanced spectral details, and enabled peak positions associated with specific components to be identified (Figure 6):

chondroitin sulfate (PG) 4310 cm^{-1}, collagen 4610 cm^{-1}, PGA 4200 cm^{-1} and water 5200 cm^{-1}. NIRS assessment of engineered cartilage samples of treated and untreated groups shows peak amplitude changes at these absorbances over time (Figure 6, 7). PGA content decreased (Figure 6A), while all tissue components including collagen (Figure 7B), PG (Figure 7C), and water (Figure 7D), increased significantly with time. For the treatment groups, we see that the only significant difference compared to the 3 week Controls was a significant increase of collagen and PG content, and decrease of PGA content, in the BMP-4/US treated group.

NIRS Correlations with MIR Compositional Measurements

A direct correlation was found between MIR and NIRS-determined PGA (R = 0.86, p = 0.02), collagen (R = 0.88, p = 0.03), and proteoglycan (R = 0.83, p = 0.01) content of the constructs. NIR-derived water content also increased with the MIR-determined PG content (R = 0.76, p = 0.04).

Mechanical Properties

The equilibrium stiffness of the Control group and BMP-4/US treated groups increased significantly between 3 and 6 weeks of culture (Figure 8A), while dynamic stiffness showed an increase in all sample groups overtime (Figure 8B). Correlations of MIR and NIR-derived matrix components with equilibrium and dynamic stiffness followed the same trend, so data are presented only for NIR-determined components and dynamic stiffness (Figures 9,10, Table 2). Data presented in Figure 9 correlate NIRS-derived measurements and mechanical stiffness for the sample groups without ultrasound treatment, while Figure 10 shows correlations for the ultrasound-treated groups. As expected, dynamic stiffness showed a negative correlation with PGA content (R = −0.71, p = 0.01), and positive correlations with water content (R = 0.74, p = 0.02), collagen content (R = 0.69, p = 0.04) and PG content (R = 0.64, p = 0.05), but only for the constructs where ultrasound was not applied (Figure 9, Table 2). Although application of ultrasound resulted in changes in matrix parameters (significantly increased collagen, Figure 7), this did not translate to improved mechanical properties (Figure 8), likely due to the increased collagen being present in the form of fibrous tissue encapsulating the periphery of the construct. In accord with this, there were no NIRS-derived compositional parameters that significantly correlated with mechanical properties in the ultrasound treated group (Figure 10, Table 2).

Discussion

Multiple tissue engineering approaches are under investigation, with techniques combining cells and biomaterials for implantation of particular interest.[72] Accordingly, longitudinal evaluation of matrix and scaffold composition is a critical step in determining appropriate compositional endpoints during development and in defining an optimal harvesting strategy. Here, the main macromolecular components of engineered tissue constructs, namely, collagen and proteoglycan, the biodegradable scaffold PGA, and water, were quantified by non-destructive NIR spectroscopy and correlated with established mid-infrared imaging spectroscopy and mechanical testing parameters. Unlike mid-IR, NIR is able to provide full-thickness data on tissue composition.

The importance of such in situ evaluation was evident from the observed dynamic evolution of construct properties over time. In the initial weeks of construct growth, chondrocytes produced matrix components that filled the interior porosities of the construct and replaced degraded PGA scaffold. Consequently, thickness was relatively constant after three weeks despite a volume increase, in accordance with previous studies.[73, 74] Histological assessment indicated heterogeneity in tissue development. At the periphery of the construct, elongated cells were found within a fibrous tissue matrix, in contrast to the hyaline-like interior regions of the tissue. This may be accounted for at least in part by differences in nutrient availability and biomechanical factors in peripheral versus central regions[75], and was particularly evident in the ultrasound treated groups. Encapsulation of BMP-4/US treated group samples by fibrous tissue, and perhaps a fibrocartilage-like tissue with reduced Alcian blue staining adjacent to the fibrous capsule, was also observed. Limited cellularity and lack of tissue production within interior regions may be due to acidity resulting from PGA degradation[76] and nutrient restriction.

Compositional changes were evaluated at microscopic pixel resolution (25 μm) by MIR spectral imaging, which enabled semi-quantitative assessment of collagen, proteoglycan (PG), and PGA.[38, 51, 52] In all groups, PGA content decreased over time, while collagen and, to a lesser extent, PG content generally increased. It is possible that the quantification of the MIR-determined PGA content was affected by the presence of scattering artifacts. However, overall, the observed trend was in accordance with what is expected, decreased PGA content over time in culture. We attribute the difference in collagen vs PG content to dedifferentiation of chondrocytes to fibroblasts or fibrochondrocyte-like cells, which produce collagen but have limited PG synthetic capability. This is consistent with the MIR images of collagen, which showed the fibrous capsule corresponding to that observed in the histology images. The overall structure and composition of these engineered cartilage constructs differ from native cartilage, although suitability for implantation may depend on factors other than similarity to native cartilage, such as maturation rate.[8] The experimental design of the present study was not targeted to assessment of constructs as implants, but rather served to identify the manner in which compositional features are reflected in NIR spectral data.

We found that NIR assessment in fiber optic mode provided a non-destructive means of evaluation of the development of engineered cartilage composition, but at significantly lower spatial resolution (~ 3.5mm) than the MIR imaging data. The NIR spectrum is dominated by peaks at 5200 cm^{-1}, 7100 cm^{-1} and 8400 cm^{-1}, arising from free water (7100cm^{-1} and 8400 cm^{-1}), and combined bound and free water (5200 cm^{-1}),[54, 56] with smaller peaks from the matrix components. It was previously shown that the area of the water peaks correlate with the amount of water present in hyaline cartilage,[56] and that the 5200 cm^{-1} peak inversely correlates with protein content.[59] However, the NIRS matrix and PGA peaks reported in this study have only recently been utilized for assessment of developing engineered cartilage[61]. The NIR absorbance near $\sim 4200 \text{ cm}^{-1}$ was found to be unique to PGA in a preliminary study [77], and here, we hypothesized that changes in this peak intensity would reflect PGA degradation. This was indeed confirmed by correlation to MIR data of PGA content. Cartilage matrix components replace degradable scaffolds over time during engineered tissue development, and the ability to monitor this process non-destructively could also be

applicable to studies where biomaterials other than PGA are used as scaffolds. For example, scaffolds frequently used in cartilage tissue engineering, such as hyaluronic acid[8], or poly (lactide-co-glycolide) (PLGA) [78], likely also have absorbances that do not overlap with the large water absorbances in the NIR spectra, and therefore would be appropriate for non-destructive monitoring of scaffold degradation.

The NIR data also correlated with gold standard MIR data, providing strong support for use of NIR for full-thickness assessment of macromolecular characterization of developing tissue-scaffold constructs. In the spectral range of interest, NIRS can provide analysis of a tissue volume on the order of several millimeters [79]. Further, unlike MIR, NIR permits ready assessment of water content. We found that although the overall percentage of gravimetrically-determined water decreased over time, the average water content of the constructs as determined by the NIR 5200 cm^{-1} peak increased. However, the former method reflects the relative percentage of water throughout the entire construct, while the NIR water peak intensity reflects the overall water content, which increases over time but to a lesser extent as the matrix portion of the constructs.

In cartilage tissue engineering, it is particularly important to have continuous full-depth longitudinal monitoring so that appropriate interventions could be introduced to augment tissue characteristics and compositional endpoints may be quantified. However, it is important to note that the current configuration of the NIR fiber optic probe does not yield spatially resolved data. Although it was possible to assess the increased collagen content in the constructs using NIR, it was not possible to observe the non-homogeneous collagen distribution. This undoubtedly contributed to the lack of correlation of the NIR matrix data with mechanical properties for the ultrasound treatment groups, where fibrous encapsulation was present. Although the specific mechanism that underlies the augmentation of the fibrous collagen in the ultrasound treatment groups is not known, these data confirm the importance of the distribution of matrix components in determination of mechanical properties of engineered constructs. It is possible that NIR fiber optics with higher resolution sampling capability could provide a solution to address this issue.

The properties of the constructs that were not treated with ultrasound developed as expected, with increasing mechanical properties over time, regardless of the addition of growth factors (Figure 9). However, although mechanical properties tended to improve over time in all sample groups studied, the equilibrium and dynamic stiffness of the engineered cartilage constructs were much lower than typical for articular cartilage,[80] even at the six week time point. It remains unknown whether harvesting should be based on chemical and cellular composition, on mechanical properties, or on other factors, such as the rate of construct development.[8] Thus, the suboptimal mechanical properties of these constructs does not necessarily preclude their use in vivo.

In summary, we have developed a non-destructive NIR spectroscopic approach to monitor engineered cartilage. Results were in very good agreement with gold standard MIR compositional analysis, and mechanical properties were predicted by NIR spectra for certain growth conditions. Our results strongly support the continued development of near infrared

spectroscopy as a non-destructive method for matrix assessment in developing engineered cartilage constructs for both *in vitro* and *in vivo* applications.

Acknowledgments

References

1. Howell DS. Pathogenesis of osteoarthritis. The American journal of medicine. 1986; 80:24. [PubMed: 3010715]

2. Moskowitz, RW. Osteoarthritis: diagnosis and medical/surgical management. Lippincott Williams & Wilkins; 2007.

3. Helmick CG, Felson DT, Lawrence RC, Gabriel S, Hirsch R, Kwoh CK, Liang MH, Kremers HM, Mayes MD, Merkel PA, Pillemer SR, Reveille JD, Stone JH. Estimates of the prevalence of arthritis and other rheumatic conditions in the United States. Part I. Arthritis Rheum. 2008; 58:15. [PubMed: 18163481]

4. Kotlarz H, Gunnarsson CL, Fang H, Rizzo JA. Insurer and out-of-pocket costs of osteoarthritis in the US: evidence from national survey data. Arthritis Rheum. 2009; 60:3546. [PubMed: 19950287]

5. Stockwell RA. The interrelationship of cell density and cartilage thickness in mammalian articular cartilage. J Anat. 1971; 109:411. [PubMed: 5153801]

6. Maroudas A, Bullough P, Swanson SA, Freeman MA. The permeability of articular cartilage. J Bone Joint Surg Br. 1968; 50:166. [PubMed: 5641590]

7. Zhou S, Cui Z, Urban JP. Factors influencing the oxygen concentration gradient from the synovial surface of articular cartilage to the cartilage-bone interface: a modeling study. Arthritis Rheum. 2004; 50:3915. [PubMed: 15593204]

8. Fisher MB, Henning EA, Soegaard NB, Dodge GR, Steinberg DR, Mauck RL. Maximizing cartilage formation and integration via a trajectory-based tissue engineering approach. Biomaterials. 2014; 35:2140. [PubMed: 24314553]

9. Hunziker EB. Articular cartilage repair: basic science and clinical progress. A review of the current status and prospects. Osteoarthritis Cartilage. 2002; 10:432. [PubMed: 12056848]

10. Buckwalter J, Mankin H. Articular cartilage. Part II: degeneration and osteoarthrosis, repair, regeneration, and transplantation. Journal of bone and joint surgery American volume. 1997; 79:612.

11. Buckwalter J, Mankin H. Articular cartilage: degeneration and osteoarthritis, repair, regeneration, and transplantation. Instructional course lectures. 1997; 47:487.

12. Temenoff JS, Mikos AG. Review: tissue engineering for regeneration of articular cartilage. Biomaterials. 2000; 21:431. [PubMed: 10674807]

13. Nakamura N, Miyama T, Engebretsen L, Yoshikawa H, Shino K. Cell-based therapy in articular cartilage lesions of the knee. Arthroscopy. 2009; 25:531. [PubMed: 19409312]

14. Buckwalter JA. Articular cartilage: injuries and potential for healing. J Orthop Sports Phys Ther. 1998; 28:192. [PubMed: 9785255]

15. Goldring MB. The role of the chondrocyte in osteoarthritis. Arthritis Rheum. 2000; 43:1916. [PubMed: 11014341]

16. Poole A. Imbalances of anabolism and catabolism of cartilage matrix components in osteoarthritis. Osteoarthritic disorders. 1995:247.

17. Danisovic L, Varga I, Zamborsky R, Bohmer D. The tissue engineering of articular cartilage: cells, scaffolds and stimulating factors. Exp Biol Med (Maywood). 2012; 237:10. [PubMed: 22156044]

18. Chung C, Burdick JA. Engineering cartilage tissue. Adv Drug Deliv Rev. 2008; 60:243. [PubMed: 17976858]

19. Frenkel SR, Di Cesare PE. Scaffolds for articular cartilage repair. Ann Biomed Eng. 2004; 32:26. [PubMed: 14964719]

20. Freed LE, Vunjak-Novakovic G, Biron RJ, Eagles DB, Lesnoy DC, Barlow SK, Langer R. Biodegradable polymer scaffolds for tissue engineering. Biotechnology (N Y). 1994; 12:689. [PubMed: 7764913]

21. Hutmacher DW. Scaffolds in tissue engineering bone and cartilage. Biomaterials. 2000; 21:2529. [PubMed: 11071603]

22. Freed LE, Marquis JC, Langer R, Vunjak-Novakovic G, Emmanual J. Composition of cell-polymer cartilage implants. Biotechnol Bioeng. 1994; 43:605. [PubMed: 18615760]

23. Blunk T, Sieminski A, Appel B, Croft C, Courter D, Chieh J, Göpferich A, Khurana J, Gooch K. Bone morphogenetic protein 9: a potent modulator of cartilage development in vitro. Growth Factors. 2003; 21:71. [PubMed: 14626354]

24. Gooch K, Blunk T, Courter D, Sieminski A, Vunjak-Novakovic G, Freed L. Bone morphogenetic proteins-2,-12, and-13 modulate in vitro development of engineered cartilage. Tissue Engineering. 2002; 8:591. [PubMed: 12201999]

25. Miljkovic N, Cooper G, Marra K. Chondrogenesis, bone morphogenetic protein-4 and mesenchymal stem cells. Osteoarthritis and Cartilage. 2008; 16:1121. [PubMed: 18406633]

26. Grunder T, Gaissmaier C, Fritz J, Stoop R, Hortschansky P, Mollenhauer J, Aicher WK. Bone morphogenetic protein (BMP)-2 enhances the expression of type II collagen and aggrecan in chondrocytes embedded in alginate beads. Osteoarthritis Cartilage. 2004; 12:559. [PubMed: 15219571]

27. Wang X, Li Y, Han R, He C, Wang G, Wang J, Zheng J, Pei M, Wei L. Demineralized bone matrix combined bone marrow mesenchymal stem cells, bone morphogenetic protein-2 and transforming growth factor-beta3 gene promoted pig cartilage defect repair. PLoS One. 2014; 9:e116061. [PubMed: 25545777]

28. Martin I, Suetterlin R, Baschong W, Heberer M, Vunjak-Novakovic G, Freed LE. Enhanced cartilage tissue engineering by sequential exposure of chondrocytes to FGF-2 during 2D expansion and BMP-2 during 3D cultivation. J Cell Biochem. 2001; 83:121. [PubMed: 11500960]

29. Freed L, Gooch K, Courter D, Blunk T, Sieminski A, Vunjak-Novakovic G. Effect of bone morphogenetic proteins on engineered cartilage. Google Patents. 2003

30. Zhang ZJ, Huckle J, Francomano CA, Spencer RG. The effects of pulsed low-intensity ultrasound on chondrocyte viability, proliferation, gene expression and matrix production. Ultrasound Med Biol. 2003; 29:1645. [PubMed: 14654159]

31. Li WJ, Tuli R, Okafor C, Derfoul A, Danielson KG, Hall DJ, Tuan RS. A three-dimensional nanofibrous scaffold for cartilage tissue engineering using human mesenchymal stem cells. Biomaterials. 2005; 26:599. [PubMed: 15282138]

32. Diekman BO, Christoforou N, Willard VP, Sun H, Sanchez-Adams J, Leong KW, Guilak F. Cartilage tissue engineering using differentiated and purified induced pluripotent stem cells. Proc Natl Acad Sci U S A. 2012; 109:19172. [PubMed: 23115336]

33. Hoemann CD, Sun J, Legare A, McKee MD, Buschmann MD. Tissue engineering of cartilage using an injectable and adhesive chitosan-based cell-delivery vehicle. Osteoarthritis Cartilage. 2005; 13:318. [PubMed: 15780645]

34. Wang L, Tran I, Seshareddy K, Weiss ML, Detamore MS. A comparison of human bone marrow-derived mesenchymal stem cells and human umbilical cord-derived mesenchymal stromal cells for cartilage tissue engineering. Tissue Eng Part A. 2009; 15:2259. [PubMed: 19260778]

35. Appel A, Anastasio MA, Brey EM. Potential for imaging engineered tissues with X-ray phase contrast. Tissue Eng Part B Rev. 2011; 17:321. [PubMed: 21682604]

36. PPBM, Pedro AJ, Peterbauer A, Gabriel C, Redl H, Reis RL. Chitosan particles agglomerated scaffolds for cartilage and osteochondral tissue engineering approaches with adipose tissue derived stem cells. J Mater Sci Mater Med. 2005; 16:1077. [PubMed: 16362204]

37. Ramaswamy S, Greco JB, Uluer MC, Zhang Z, Fishbein KW, Spencer RG. Magnetic resonance imaging of chondrocytes labeled with superparamagnetic iron oxide nanoparticles in tissue-engineered cartilage. Tissue Eng Part A. 2009; 15:3899. [PubMed: 19788362]

38. Reiter DA, Irrechukwu O, Lin PC, Moghadam S, Von Thaer S, Pleshko N, Spencer RG. Improved MR-based characterization of engineered cartilage using multiexponential T2 relaxation and multivariate analysis. NMR Biomed. 2012; 25:476. [PubMed: 22287335]

39. Keeney M, Lai JH, Yang F. Recent progress in cartilage tissue engineering. Curr Opin Biotechnol. 2011; 22:734. [PubMed: 21531126]

40. Little CJ, Bawolin NK, Chen X. Mechanical properties of natural cartilage and tissue-engineered constructs. Tissue Eng Part B Rev. 2011; 17:213. [PubMed: 21406046]

41. Dumas D, Riquelme B, Werkmeister E, Isla N, Stoltz JF. Multimodality of microscopy imaging applied to cartilage tissue engineering. BIOMEDICAL AND HEALTH RESEARCH-COMMISSION OF THE EUROPEAN COMMUNITIES THEN IOS PRESS. 2007; 70:254.

42. Zhang Z, McCaffery JM, Spencer RG, Francomano CA. Hyaline cartilage engineered by chondrocytes in pellet culture: histological, immunohistochemical and ultrastructural analysis in comparison with cartilage explants. Journal of anatomy. 2004; 205:229. [PubMed: 15379928]

43. Hoemann, CD. Cartilage and osteoarthritis. Springer; 2004. Molecular and biochemical assays of cartilage components; p. 127-156.

44. Hoemann CD, Sun J, Chrzanowski V, Buschmann MD. A multivalent assay to detect glycosaminoglycan, protein, collagen, RNA, and DNA content in milligram samples of cartilage or hydrogel-based repair cartilage. Anal Biochem. 2002; 300:1. [PubMed: 11743684]

45. Peretti GM, Randolph MA, Zaporojan V, Bonassar LJ, Xu JW, Fellers JC, Yaremchuk MJ. A biomechanical analysis of an engineered cell-scaffold implant for cartilage repair. Ann Plast Surg. 2001; 46:533. [PubMed: 11352428]

46. Martin I, Obradovic B, Treppo S, Grodzinsky AJ, Langer R, Freed LE, Vunjak-Novakovic G. Modulation of the mechanical properties of tissue engineered cartilage. Biorheology. 2000; 37:141. [PubMed: 10912186]

47. Yang Y, Dubois A, Qin XP, Li J, El Haj A, Wang RK. Investigation of optical coherence tomography as an imaging modality in tissue engineering. Phys Med Biol. 2006; 51:1649. [PubMed: 16552095]

48. Rice MA, Waters KR, Anseth KS. Ultrasound monitoring of cartilaginous matrix evolution in degradable PEG hydrogels. Acta Biomater. 2009; 5:152. [PubMed: 18793879]

49. Kotecha M, Klatt D, Magin RL. Monitoring cartilage tissue engineering using magnetic resonance spectroscopy, imaging, and elastography. Tissue Eng Part B Rev. 2013; 19:470. [PubMed: 23574498]

50. Irrechukwu ON, Lin PC, Fritton K, Doty S, Pleshko N, Spencer RG. Magnetic resonance studies of macromolecular content in engineered cartilage treated with pulsed low-intensity ultrasound. Tissue Eng Part A. 2011; 17:407. [PubMed: 20807015]

51. West PA, Bostrom MP, Torzilli PA, Camacho NP. Fourier transform infrared spectral analysis of degenerative cartilage: an infrared fiber optic probe and imaging study. Appl Spectrosc. 2004; 58:376. [PubMed: 15104805]

52. Boskey A, Camacho NP. FT-IR imaging of native and tissue-engineered bone and cartilage. Biomaterials. 2007; 28:2465. [PubMed: 17175021]

53. Hanifi A, Richardson JB, Kuiper JH, Roberts S, Pleshko N. Clinical outcome of autologous chondrocyte implantation is correlated with infrared spectroscopic imaging-derived parameters. Osteoarthritis and Cartilage. 2013; 20:988.

54. Afara I, Singh S, Oloyede A. Application of near infrared (NIR) spectroscopy for determining the thickness of articular cartilage. Med Eng Phys. 2013; 35:88. [PubMed: 22824725]

55. Padalkar M, Pleshko N. Wavelength-dependent penetration depth of near infrared radiation into cartilage. Analyst. 2015; 140:2093. [PubMed: 25630381]

56. Padalkar MV, Spencer RG, Pleshko N. Near Infrared Spectroscopic Evaluation of Water in Hyaline Cartilage. Annals of Biomedical Engineering. 2013; 41:2426. [PubMed: 23824216]

57. Spahn G, Plettenberg H, Nagel H, Kahl E, Klinger HM, Muckley T, Gunther M, Hofmann GO, Mollenhauer JA. Evaluation of cartilage defects with near-infrared spectroscopy (NIR): an ex vivo study. Med Eng Phys. 2008; 30:285. [PubMed: 17553725]

58. Hofmann GO, Marticke J, Grossstuck R, Hoffmann M, Lange M, Plettenberg HK, Braunschweig R, Schilling O, Kaden I, Spahn G. Detection and evaluation of initial cartilage pathology in man: A comparison between MRT, arthroscopy and near-infrared spectroscopy (NIR) in their relation to initial knee pain. Pathophysiology. 2010; 17:1. [PubMed: 19481428]

59. Baykal D, Irrechukwu O, Lin PC, Fritton K, Spencer RG, Pleshko N. Nondestructive Assessment of Engineered Cartilage Constructs Using Near-Infrared Spectroscopy. Applied Spectroscopy. 2010; 64:1160. [PubMed: 20925987]

60. Palukuru UP, McGoverin CM, Pleshko N. Assessment of hyaline cartilage matrix composition using near infrared spectroscopy. Matrix Biology. 2014; 38:3. [PubMed: 25083813]

61. McGoverin CM, Hanifi A, Palukuru UP, Yousefi F, Glenn PB, Shockley M, Spencer RG, Pleshko N. Non-destructive Assessment of Engineered Cartilage Composition by Near Infrared Spectroscopy. Ann Biomed Eng. 2016

62. Kister G, Cassanas G, Vert M. Morphology of poly (glycolic acid) by IR and Raman spectroscopies. Spectrochimica Acta Part A: Molecular and Biomolecular Spectroscopy. 1997; 53:1399.

63. West PA, Torzilli PA, Chen C, Lin P, Camacho NP. Fourier transform infrared imaging spectroscopy analysis of collagenase-induced cartilage degradation. J Biomed Opt. 2005; 10:14015. [PubMed: 15847596]

64. Camacho NP, West P, Torzilli PA, Mendelsohn R. FTIR microscopic imaging of collagen and proteoglycan in bovine cartilage. Biopolymers. 2001; 62:1. [PubMed: 11135186]

65. Bychkov SM, Bogatov VN, Kharlamova VN. Infrared spectra of certain proteoglycans. Biull Eksp Biol Med. 1980; 89:680. [PubMed: 7397357]

66. Rinnan Å, Berg Fvd, Engelsen SB. Review of the most common pre-processing techniques for near-infrared spectra. TrAC Trends in Analytical Chemistry. 2009; 28:1201.

67. Rieppo L, Saarakkala S, Närhi T, Helminen H, Jurvelin J, Rieppo J. Application of second derivative spectroscopy for increasing molecular specificity of fourier transform infrared spectroscopic imaging of articular cartilage. Osteoarthritis and Cartilage. 2012; 20:451. [PubMed: 22321720]

68. Shockley, M., McGoverin, C., Palukuru, U., Glenn, P., Spencer, R., Pleshko, N. Near Infrared Spectroscopy as a Method for Non-destructive Monitoring of Engineered Cartilage Growth. 39th Annual Northeast Bioengineering Conference; Syracuse, NY: SYRACUSE UNIVERSITY; IEEE; 2013. p. 51-52.

69. Park S, Nicoll SB, Mauck RL, Ateshian GA. Cartilage mechanical response under dynamic compression at physiological stress levels following collagenase digestion. Ann Biomed Eng. 2008; 36:425. [PubMed: 18193355]

70. Sah RL, Kim YJ, Doong JY, Grodzinsky AJ, Plaas AH, Sandy JD. Biosynthetic response of cartilage explants to dynamic compression. J Orthop Res. 1989; 7:619. [PubMed: 2760736]

71. Vunjak-Novakovic G, Martin I, Obradovic B, Treppo S, Grodzinsky AJ, Langer R, Freed LE. Bioreactor cultivation conditions modulate the composition and mechanical properties of tissue-engineered cartilage. J Orthop Res. 1999; 17:130. [PubMed: 10073657]

72. Appel AA, Anastasio MA, Larson JC, Brey EM. Imaging challenges in biomaterials and tissue engineering. Biomaterials. 2013; 34:6615. [PubMed: 23768903]

73. Erickson IE, Kestle SR, Zellars KH, Dodge GR, Burdick JA, Mauck RL. Improved cartilage repair via in vitro pre-maturation of MSC-seeded hyaluronic acid hydrogels. Biomed Mater. 2012; 7:024110. [PubMed: 22455999]

74. Erickson IE, Kestle SR, Zellars KH, Farrell MJ, Kim M, Burdick JA, Mauck RL. High mesenchymal stem cell seeding densities in hyaluronic acid hydrogels produce engineered cartilage with native tissue properties. Acta Biomater. 2012; 8:3027. [PubMed: 22546516]

75. Moutos FT, Guilak F. Composite scaffolds for cartilage tissue engineering. Biorheology. 2008; 45:501. [PubMed: 18836249]

76. Oliveira JT, Crawford A, Mundy JM, Moreira AR, Gomes ME, Hatton PV, Reis RL. A cartilage tissue engineering approach combining starch-polycaprolactone fibre mesh scaffolds with bovine articular chondrocytes. J Mater Sci Mater Med. 2007; 18:295. [PubMed: 17323161]

77. Shockley, M., McGoverin, C., Palukuru, U., Glenn, P., Spencer, R., Pleshko, N. Near Infrared Spectroscopy as a Method for Non-destructive Monitoring of Engineered Cartilage Growth. 39th Annual Northeast Bioengineering Conference; 2013. p. 51

78. Wang W, Li B, Li Y, Jiang Y, Ouyang H, Gao C. In vivo restoration of full-thickness cartilage defects by poly(lactide-co-glycolide) sponges filled with fibrin gel, bone marrow mesenchymal stem cells and DNA complexes. Biomaterials. 2010; 31:5953. [PubMed: 20488531]

79. Padalkar MV, Pleshko N. Wavelength-dependent penetration depth of near infrared radiation into cartilage. Analyst. 2015; 140:2093. [PubMed: 25630381]

80. Park S, Hung CT, Ateshian GA. Mechanical response of bovine articular cartilage under dynamic unconfined compression loading at physiological stress levels. Osteoarthritis Cartilage. 2004; 12:65. [PubMed: 14697684]

3 Weeks **6 Weeks**

Control

5 mm 5 mm

BMP-4/US

5 mm 5 mm
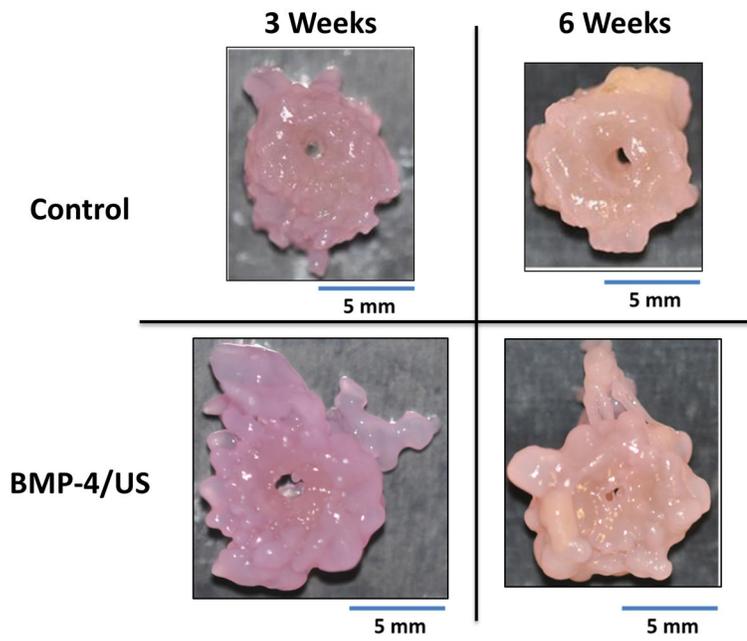
Fig. 1.
A representative Control and BMP-4/US treated engineered cartilage construct. A color difference from red to light pink is visible in the construct from week 3 to week 6 of tissue culture, due to varying amounts of media absorbed.
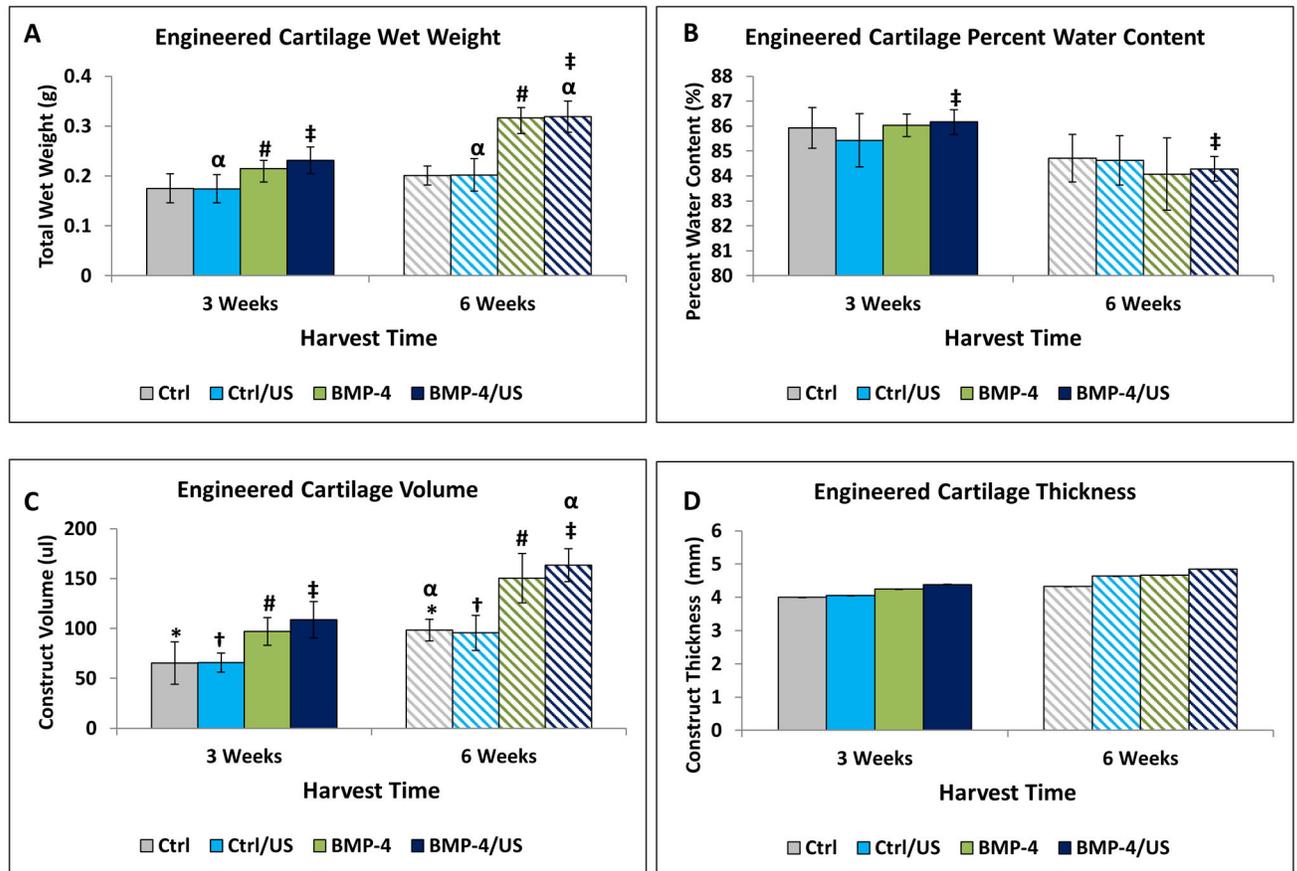
Fig. 2.
Tissue development of engineered cartilage constructs (obtained from the half constructs prior to mechanical testing) over time. Construct water content increased from week 3 to week 6 for all sample groups (A), but due to the simultaneous increase in dry weight, the water percentage decreased (B). Radial expansion of constructs increased the tissue volume (C) while the thickness remained the same (D). Symbols show statistical significance at $p < 0.05$, with matching symbols indicating significance between groups.
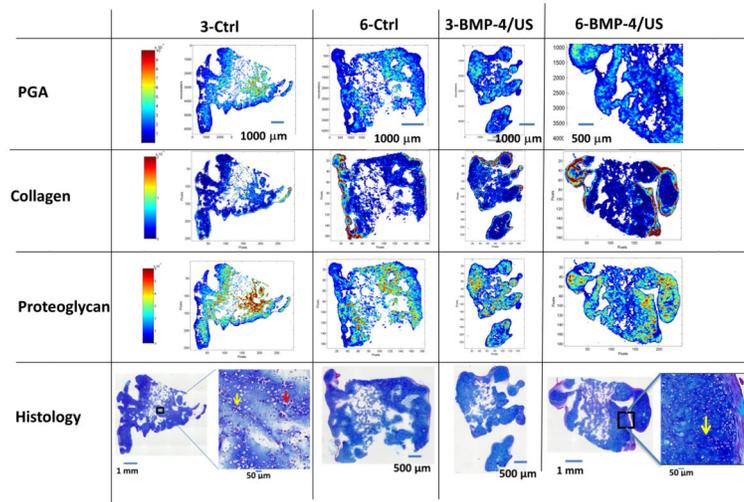
Fig. 3.
MIR spectral imaging-derived PGA, collagen and PG. Alcian blue and H&E co-staining assessment of Control and BMP-4/US treated samples in week 3 and week 6 of the same tissue sections are included for comparison. In agreement with Alcian blue staining in histology images, the PG distribution can be seen throughout the tissue in the MIR images. There is a high concentration of collagen in the periphery due to the production of a fibrous capsule around the tissue, and flattened cells are present (blue arrow). Chondrocytes appear in their native-like lacunae (yellow arrow), and in week 3 images there are still PGA fibers left in the construct (red arrow).
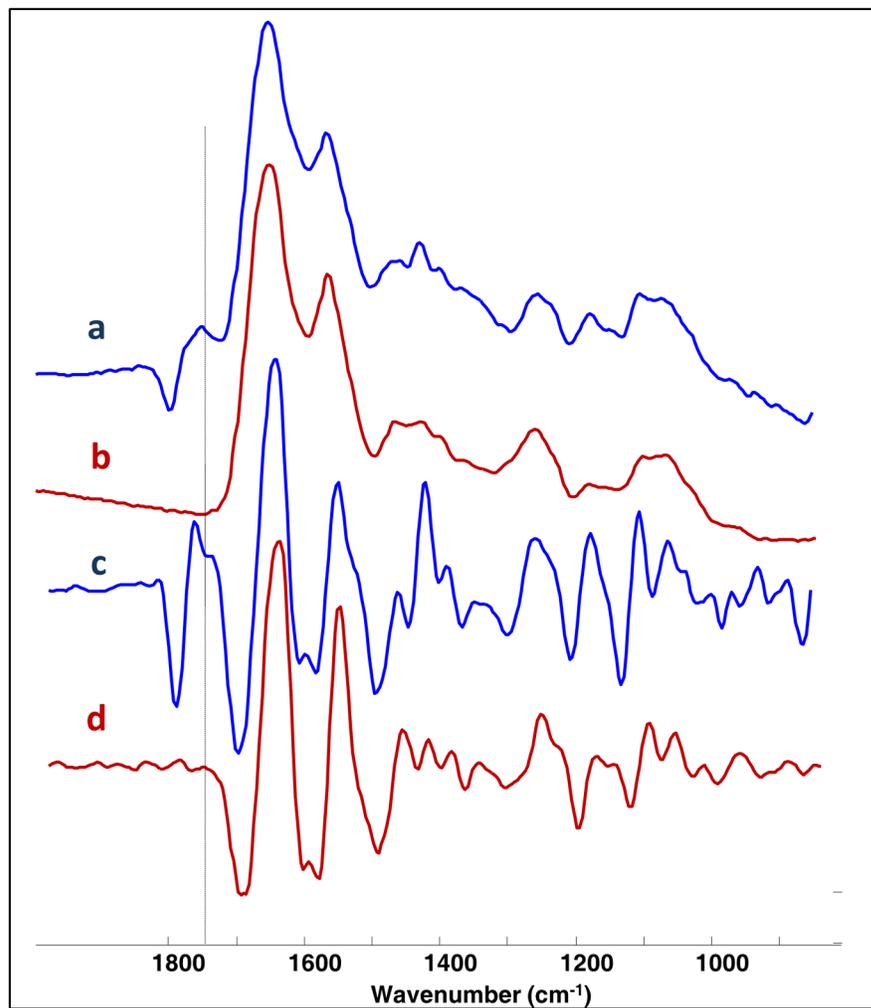
Fig. 4.
(A). Raw, MSC-corrected (a,b) and second derivative (c,d) spectra obtained from regions of engineered constructs with (a,c) and without (b,d) residual PGA. Scattering artifacts are evident in the spectra just above the PGA absorbance at ~ 1748 cm^{-1}.
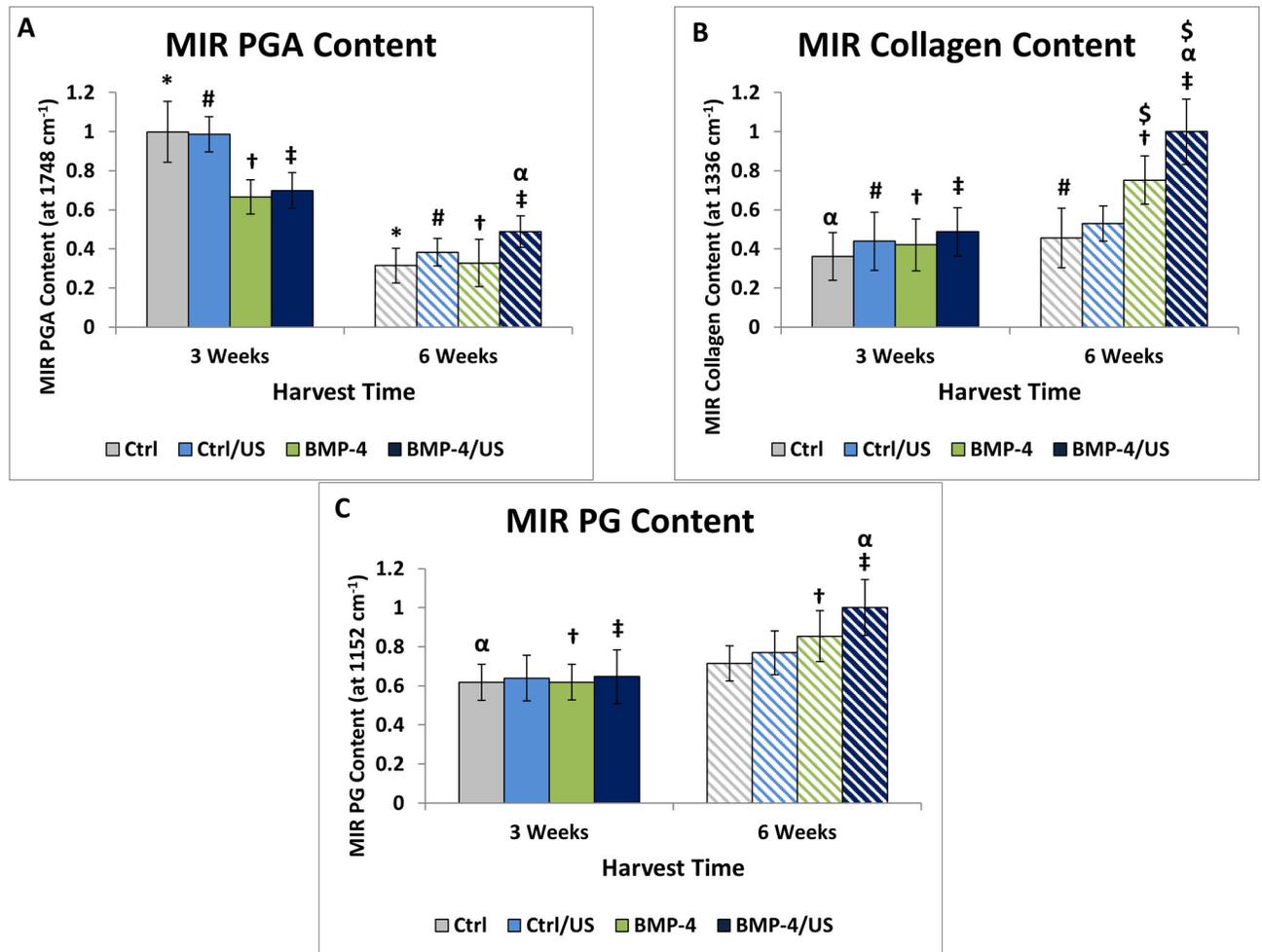
Fig. 5.

MIR semi-quantitative measurements of PGA (A), collagen (B), and PG (C). PGA decreased from 3 to 6 weeks, and collagen and PG increased. PGA and collagen variations are significantly different among all sample groups, while there is only a significant difference between Control and BMP-4/US treated samples PG content. Symbols show statistical significance at p < 0.05, with matching symbols indicating significance between groups.
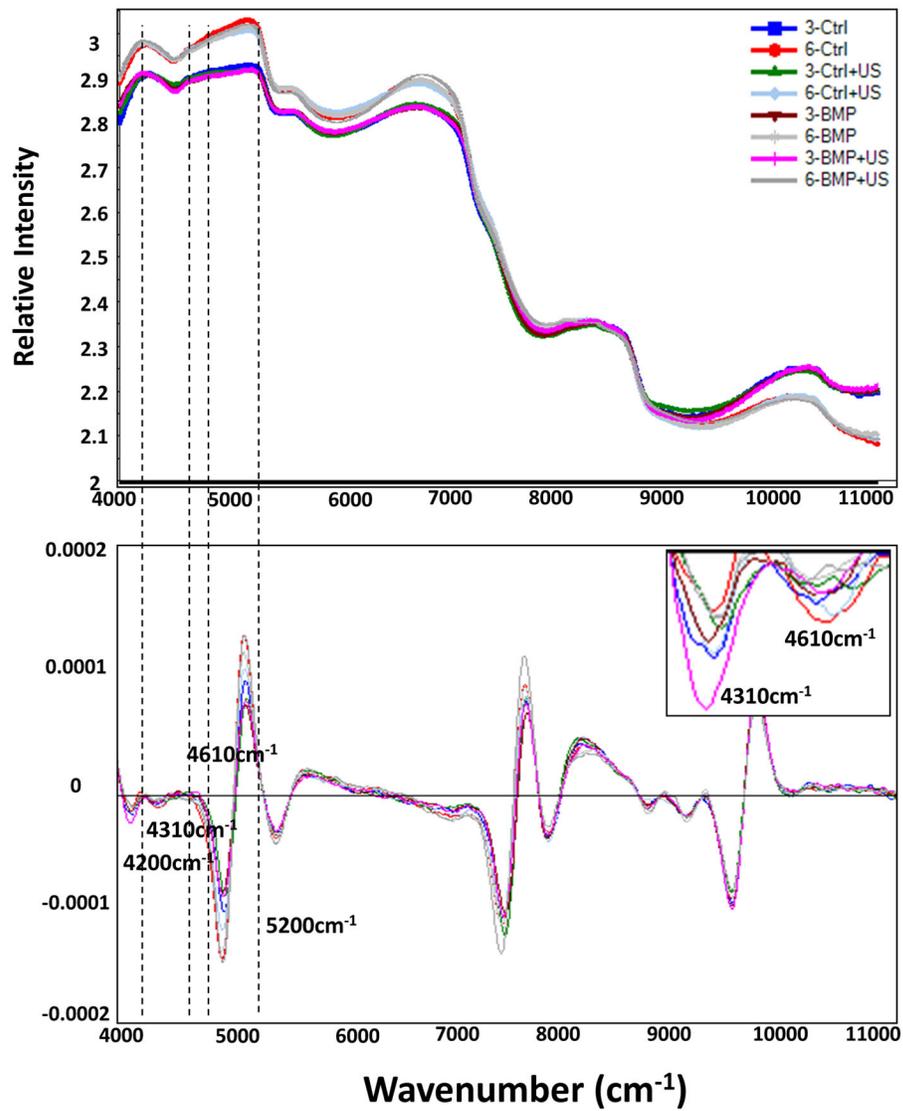
Fig. 6.
NIR raw spectra (top) and smoothed second derivative spectra (B) showing peak height differences at water (5200 cm^{-1}), PG (4310 cm^{-1}), PGA (4200 cm^{-1}), and collagen (4610 cm^{-1})-related absorbances.
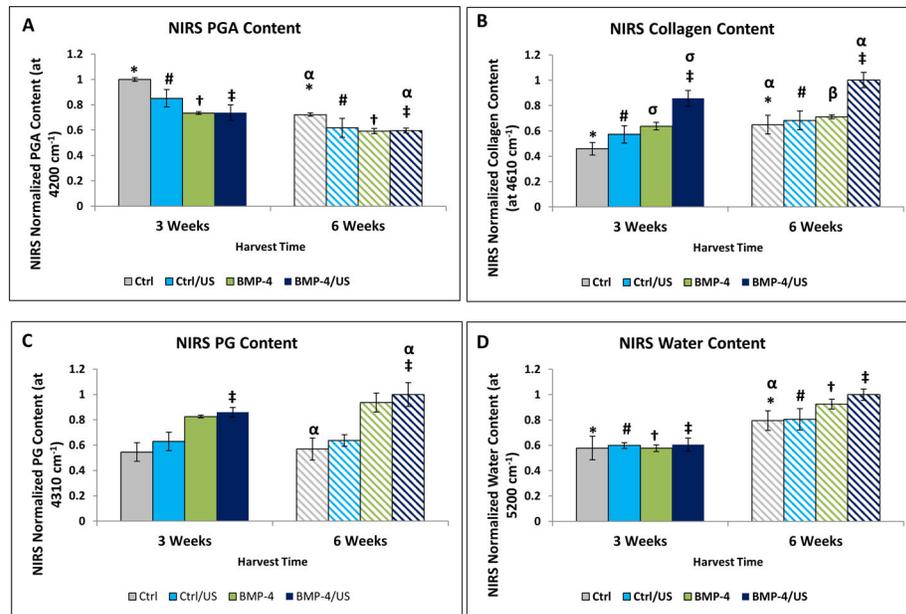
Fig. 7.
NIRS-derived matrix components measuring A) PGA (4200 cm^{-1}), B) Collagen (4610 cm^{-1}), C) PG (4310 cm^{-1}), and D) water (5200 cm^{-1}). There is a significant difference between water, PGA, and collagen content from 3 to 6 weeks harvest time points, and in the BMP-4 groups compared to the BMP-4/US at the same timepoints ($p < 0.05$). PG content generally increases over time, but only the BMP-4/US treated group shows a significance difference compared to Control (C). Symbols show statistical significance at $p < 0.05$, with matching symbols indicating significance between groups.
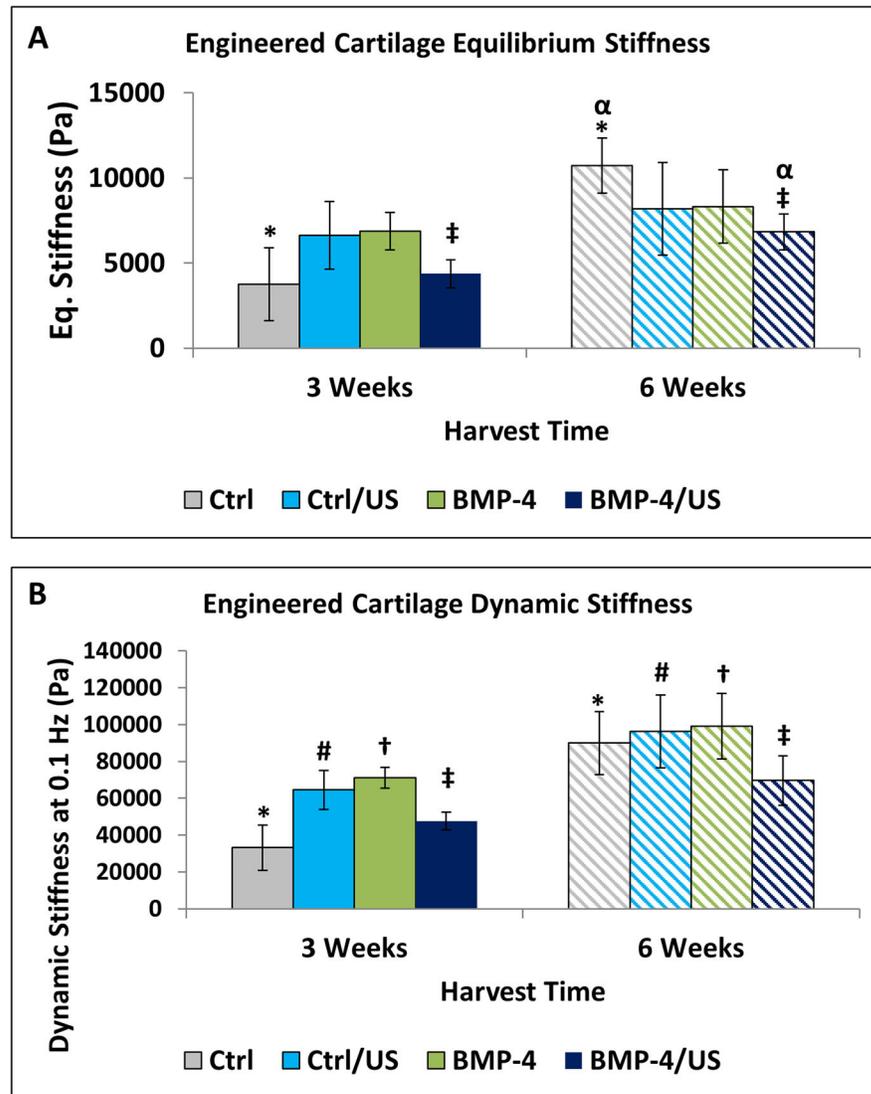
Fig. 8.
Equilibrium (A) and dynamic (B) stiffness of engineered cartilage calculated for all sample groups. Dynamic stiffness is only shown for the 0.1 Hz frequency since all frequencies had a similar pattern. Over time the construct stiffness generally increased. Symbols show statistical significance at $p < 0.05$, with matching symbols indicating significance between groups.
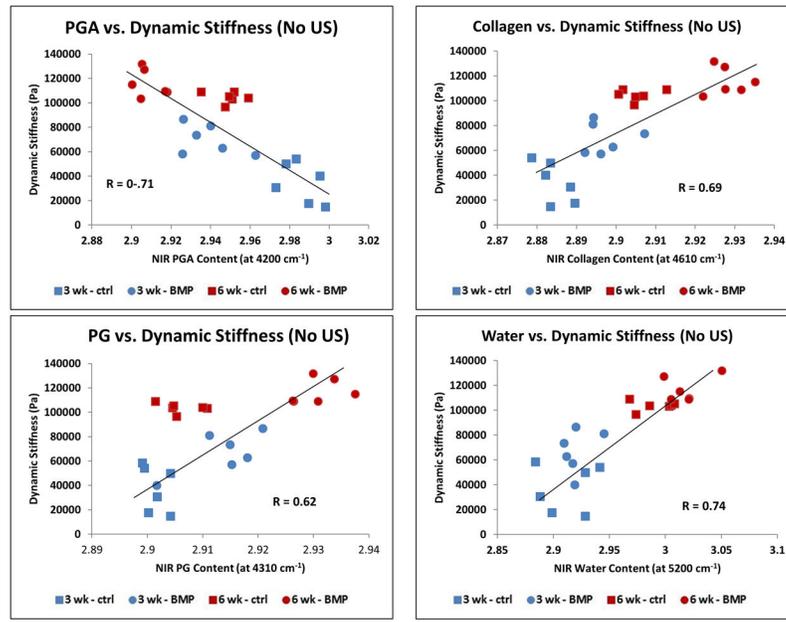
Fig. 9.
Correlation of NIRS-derived cartilage matrix components for combined control and BMP-4 treated groups at 3 and 6 weeks of growth with dynamic stiffness: PGA (A), Collagen (B), PG (C), and water (D). All correlations were significant (Table 2).
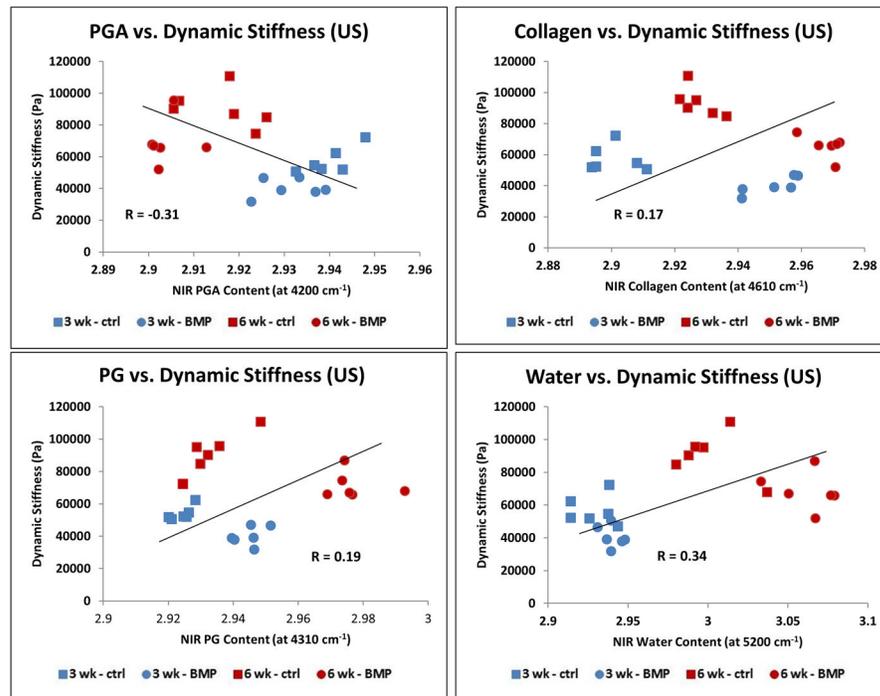
Fig. 10.
Correlation of NIRS-derived cartilage matrix components for combined control/US and BMP-4/US treated groups at 3 and 6 weeks of growth with dynamic stiffness: PGA (A), Collagen (B), PG (C), and water (D). There were no significant correlations (Table 2).

Table 1

Sample groups based on harvest time and treatment.

Sample Group Name (N = 6 per group)	Treatment
3 Weeks - Ctrl	-
3 Weeks - Ctrl/US	Ultrasound
3 Weeks – BMP4	BMP-4
3 Weeks – BMP4/US	BMP-4 and Ultrasound
6 Weeks - Ctrl	-
6 Weeks - Ctrl/US	Ultrasound
6 Weeks – BMP4	BMP-4
6 Weeks – BMP4/US	BMP-4 and Ultrasound

Table 2

Correlation of NIRS Parameters with Dynamic Stiffness

No US (N = 24)	R	p
Water	0.74	0.02
PGA	0.71	0.01
Collagen	0.69	0.04
PG	0.62	0.05
With US (N = 24)	**R**	**p**
Water	0.34	0.2
PGA	0.31	0.3
Collagen	0.17	0.5
PG	0.19	0.4